Unnatural verticilide enantiomer inhibits type 2 ryanodine receptor-mediated calcium leak and is antiarrhythmic

Suzanne M. Batiste[a,1], Daniel J. Blackwell[b,1], Kyungsoo Kim[b,1], Dmytro O. Kryshtal[b], Nieves Gomez-Hurtado[b], Robyn T. Rebbeck[c], Razvan L. Cornea[c], Jeffrey N. Johnston[a,2], and Bjorn C. Knollmann[b,2]

[a]Department of Chemistry, Vanderbilt University, Nashville, TN 37235; [b]Department of Medicine, Vanderbilt University Medical Center, Nashville, TN 37232; and [c]Department of Biochemistry, Molecular Biology, and Biophysics, University of Minnesota, Minneapolis, MN 55455

Edited by Dale L. Boger, The Scripps Research Institute, La Jolla, CA, and approved January 15, 2019 (received for review September 27, 2018)

Ca^{2+} leak via ryanodine receptor type 2 (RyR2) can cause potentially fatal arrhythmias in a variety of heart diseases and has also been implicated in neurodegenerative and seizure disorders, making RyR2 an attractive therapeutic target for drug development. Here we synthesized and investigated the fungal natural product and known insect RyR antagonist (−)-verticilide and several congeners to determine their activity against mammalian RyR2. Although the cyclooligomeric depsipeptide natural product (−)-verticilide had no effect, its nonnatural enantiomer [*ent*-(+)-verticilide] significantly reduced RyR2-mediated spontaneous Ca^{2+} leak both in cardiomyocytes from wild-type mouse and from a gene-targeted mouse model of Ca^{2+} leak-induced arrhythmias (*Casq2*$^{-/-}$). *ent*-(+)-verticilide selectively inhibited RyR2-mediated Ca^{2+} leak and exhibited higher potency and a distinct mechanism of action compared with the pan-RyR inhibitors dantrolene and tetracaine and the antiarrhythmic drug flecainide. *ent*-(+)-verticilide prevented arrhythmogenic membrane depolarizations in cardiomyocytes without significant effects on the cardiac action potential and attenuated ventricular arrhythmia in catecholamine-challenged *Casq2*$^{-/-}$ mice. These findings indicate that *ent*-(+)-verticilide is a potent and selective inhibitor of RyR2-mediated diastolic Ca^{2+} leak, making it a molecular tool to investigate the therapeutic potential of targeting RyR2 hyperactivity in heart and brain pathologies. The enantiomer-specific activity and straightforward chemical synthesis of (unnatural) *ent*-(+)-verticilide provides a compelling argument to prioritize *ent*-natural product synthesis. Despite their general absence in nature, the enantiomers of natural products may harbor unprecedented activity, thereby leading to new scaffolds for probe and therapeutic development.

natural product | ryanodine receptor | CPVT | cardiomyocytes | depsipeptide

The ryanodine receptor (RyR) is an intracellular Ca^{2+} release channel that plays a critical role in excitable tissue. Mammals have three isoforms: RyR1 and RyR2, which are abundantly expressed in skeletal and cardiac muscle, respectively, and RyR3, which has a broad expression profile. Neuronal expression of RyR varies, but RyR2 is most abundant. In the brain, spontaneous Ca^{2+} leak via RyR2 is implicated in a number of disorders, including Alzheimer's disease, memory loss (1), neurodegeneration, and seizures (2, 3). The pan-RyR inhibitor, dantrolene, has been shown to be neuroprotective in mouse models of Huntington's disease (4), cerebral ischemia (5), and spinocerebellar ataxia type 2 and 3 (6, 7), suggesting a direct role for RyR2-mediated Ca^{2+} leak. This field is underexplored, however, because no RyR2-selective inhibitor currently exists.

In the heart, RyR2 mediates excitation–contraction (EC) coupling, and opening of RyR2 channels is tightly regulated (8). Abnormally high RyR2 activity during diastole causes EC coupling-independent spontaneous intracellular Ca^{2+} release from the sarcoplasmic reticulum (SR) and has been documented in human heart diseases associated with both atrial and ventricular arrhythmia (9). Mutations in RyR2 and its binding partners, which increase SR Ca^{2+} leak, cause primary atrial and ventricular arrhythmia syndromes such as catecholaminergic polymorphic ventricular tachycardia (CPVT), providing strong evidence for the mechanistic contribution of RyR2 to arrhythmia risk in humans (10). Further support comes from gene-targeted mouse models of CPVT, where catecholamine-induced spontaneous Ca^{2+} release from the SR via RyR2 generates potentially fatal cardiac arrhythmias (11, 12). Previously, we discovered that an antiarrhythmic small molecule drug currently in clinical use, flecainide (Fig. 1), reduced CPVT episodes both in a calsequestrin knockout (*Casq2*$^{-/-}$) mouse model of CPVT and in CPVT patients (13). Flecainide effectively suppresses RyR2-mediated spontaneous Ca^{2+} release in CPVT cardiomyocytes (isolated cardiac cells) independent of its action as a Na^{+} channel blocker (13, 14), even though recent work suggests that the flecainide mode of action (MOA) is difficult to explain based on studies of single RyR2 channels incorporated in artificial lipid bilayers (15). On the other hand, dantrolene, a non-selective RyR inhibitor approved for clinical use against skeletal muscle spasticity and malignant hyperthermia (16), potently inhibits single RyR2 channels (17) but is much less potent in [^{3}H]ryanodine RyR2 binding assays (18) and has limited efficacy in vivo against CPVT (19). Therefore, new small-molecule tool compounds are

Significance

This report highlights a rare and exciting discovery of an unnatural enantiomer of a natural product [a cyclooligomeric depsipeptide (COD)] that potently inhibits ryanodine receptor type 2 (RyR2), a target for therapeutic development for which there are no known selective inhibitors. To our knowledge, there are no examples where the unnatural enantiomer of a natural product is highly potent at its protein target while the natural enantiomer is inactive. This discovery raises the question whether the enantiomers of other natural products harbor potent biological activity but will remain undiscovered until they are prepared or, alternatively, a mirror-image protein is used to screen natural product libraries.

Author contributions: S.M.B., D.J.B., K.K., N.G.-H., R.T.R., R.L.C., J.N.J., and B.C.K. designed research; S.M.B., D.J.B., K.K., D.O.K., N.G.-H., and R.T.R. performed research; S.M.B., D.J.B., K.K., N.G.-H., R.T.R., R.L.C., J.N.J., and B.C.K. analyzed data; and S.M.B., D.J.B., R.L.C., J.N.J., and B.C.K. wrote the paper.

The authors declare no conflict of interest.

This article is a PNAS Direct Submission.

[1]S.M.B., D.J.B., and K.K. contributed equally to this work.

[2]To whom correspondence may be addressed. Email: jeffrey.n.johnston@vanderbilt.edu or bjorn.knollmann@vanderbilt.edu.

This article contains supporting information online at www.pnas.org/lookup/suppl/doi:10.1073/pnas.1816685116/-/DCSupplemental.

Published online February 21, 2019.

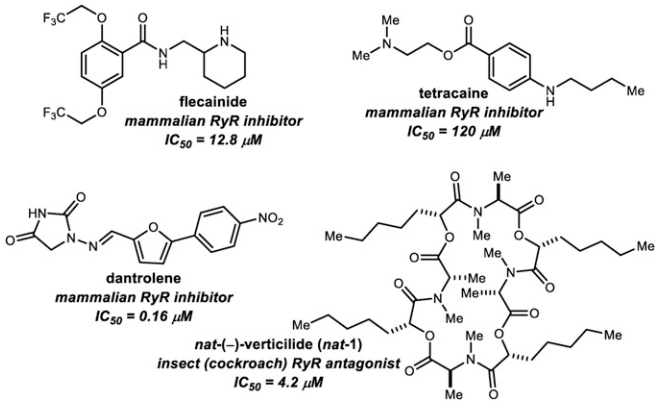

Fig. 1. Small-molecule RyR modulators.

needed to understand regulation of cellular Ca^{2+} flux and its potential as a pharmacologic target for the prevention of cardiac arrhythmias triggered by untimely Ca^{2+} release through RyR2 channels.

Natural products often serve as an excellent discovery platform to uncover new chemical tools because they can provide diverse molecular architectures and immediate accessibility in amounts often sufficient to examine initial biological activity (22). In most cases, chiral natural products are produced biosynthetically as a single enantiomer but in rare cases can be produced as both enantiomers in a racemic mixture or as the opposite enantiomer from a different species (23). The two mirror image isomers have identical chemical properties but often exhibit different biological functions or activities (24, 25), which makes them effective discovery tools to study stereodifferentiated interactions between these complex small molecules and a targeted biomolecule. (−)-Verticilide (*nat*-**1**) is a fungal cyclooligomeric depsipeptide (COD) natural product, derived from alternating α-hydroxy acid and α-amino acid monomers. Fungal CODs are structurally privileged natural products as demonstrated by their broad spectrum of biological activities, including antibiotic, insecticidal, and antitumor activities (26). Some CODs bind ions (27, 28) and serve as transporters across cell membranes—a feature which may contribute to their bioactivity (26). Additionally, they have a number of structural features, such as ring size, degree of *N*-methylation, α-amino acid and α-hydroxy acid sidechains, and respective D- and L-stereochemistry, which can modulate their bioactivity (29, 30). However, biosynthetic structural diversification is limited because fungal COD-producing nonribosomal peptide synthetases (NRPSs) are only capable of incorporating a limited number of side chains (31). Moreover, fungal NRPSs selectively activate a specific enantiomer in the condensation domain from a racemic mixture to be coupled with the next in the sequence (32, 33), leading to only one of two possible enantiomers produced naturally. Unlike terpene or polyketide natural products, which can be found in nature as the racemate or as an organism-specific single enantiomer (23), the enantiomeric pair to a fungal COD natural product must be accessed by chemical synthesis. Unfortunately, traditional chemical synthesis of CODs remains a challenging, slow process in many cases (26). As a consequence, the biological relevance of *ent*-COD natural products and other derivatives is underexplored. We report the discovery of potent biological activity and therapeutic potential of an unnatural small molecule, *ent*-(+)-verticilide, that contrasts the inactivity of its mirror image, (−)-verticilide, a naturally occurring COD.

Methods

Details of the synthesis, purification, and characterization of all new compounds, including NMR spectra, are provided in *SI Appendix*. The use of animals was approved by the Animal Care and Use Committee of Vanderbilt University. RyR2 function was assayed using [^{3}H]ryanodine binding (20) and Ca^{2+} spark assays (21). Drug effects on arrhythmia were tested in cardiomyocytes isolated from $Casq2^{-/-}$ mice and in vivo using a catecholamine challenge (13). An expanded method section is in *SI Appendix*.

Results and Discussion

(−)-Verticilide (*nat*-**1**; Fig. 1) was first isolated in 2006 (34, 35) from a culture broth of *Verticillium* sp. FKI-1033 by Ōmura and coworkers while screening for potential insecticides. Its structure was determined to be a 24-membered COD consisting of alternating (+)-(*R*)-2-hydroxyheptanoic acid and *N*-methyl-L-alanine residues. *nat*-(−)-verticilide was found to be an RyR antagonist, inhibiting insect RyR with an IC_{50} value of 4.2 μM (35). Because insects have only one RyR isoform, (−)-verticilide is a promising lead for developing new insecticides (36). (−)-Verticilide weakly inhibits mouse RyR1 with an IC_{50} value of 53.9 μM (35), but its affinity to mammalian RyR2 or RyR3 is unknown. Given its known RyR activity, we hypothesized that verticilide may also act on mammalian RyR2.

Two approaches to the synthesis of verticilide were leveraged to obtain verticilide congeners needed to investigate structure-related activity against RyR2. First, *nat*-(−)-verticilide was synthesized using a macrocyclodimerization approach from tetradepsipeptide *seco*-acid **3** in an eight-step longest linear sequence (37). To obtain a linear precursor to verticilide, the synthesis was diverted from common tetradepsipeptide intermediate **2** to ultimately access **7** through a series of convergent deprotection and coupling steps (Scheme 1). Finally, **7** was subjected to Mitsunobu macrocyclization conditions to afford the 24-membered N–H precursor **8**, which was transformed to *nat*-(−)-verticilide by per-*N*-methylation. Additionally, this simple, rapidly executed platform was used to prepare mirror image isomers *ent*-**7**, *ent*-**8**, and *ent*-(+)-verticilide (*ent*-**1**) in pure form from *ent*-**2** (Scheme 1, blue *Inset*).

Cardiomyocyte (heart cell) studies of the functional effects of natural-(−)- and unnatural *ent*-(+)-verticilide and their N–H congeners on RyR2 activity were performed using a *Casq*2 gene knockout ($Casq2^{-/-}$) mouse, which is a validated model of severe human CPVT that exhibits pathologically increased RyR2 activity (10). Ventricular cardiomyocytes were isolated, permeabilized with saponin to enable equivalent access of the compounds to the SR membrane, and incubated with vehicle (DMSO) or 25 μM *nat*- and *ent*-**1**, **7**, and **8**. RyR2 activity was measured in the form of Ca^{2+} sparks, which are elementary Ca^{2+} release events generated by spontaneous openings of intracellular RyR2 Ca^{2+} release channels (21). Fig. 2*A* shows representative confocal line scans for cells treated with DMSO, *nat*-**1**, or *ent*-**1**. Whereas *nat*-**1** and the synthetic precursors had no effect on Ca^{2+} sparks, *ent*-**1** significantly reduced spark frequency (Fig. 2*B*), indicating that

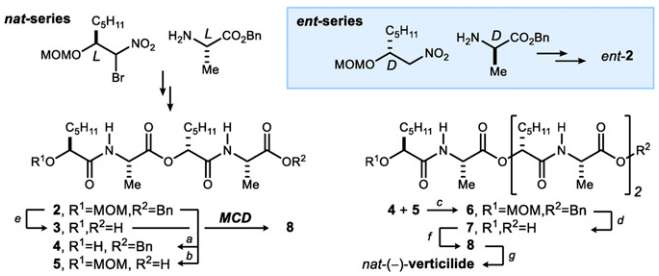

Scheme 1. Macrocyclo-dimerization (MCD) (37) and modular convergent routes to verticilide: (a) $BF_3{\bullet}OEt_2$, PhSH, CH_2Cl_2, rt, 85%; (b) H_2, Pd/C, EtOH/CH_2Cl_2 (10:1), rt, 97%; (c) DIAD, PPh_3, benzene, rt, 93%; (d) $AlCl_3$, CH_3NO_2, 0 °C → rt, 97%; (e) $AlCl_3$, CH_2Cl_2, 0 °C → rt, 97%; (f) DIAD, PPh_3, benzene, rt, 80%; (MCD) (37) DIAD, PPh_3, $NaBF_4$, benzene, rt, 89%; and (g) NaH, MeI, DMF, 0 °C, 78%. MOM, methoxy methylene ether; Bn, benzyl.

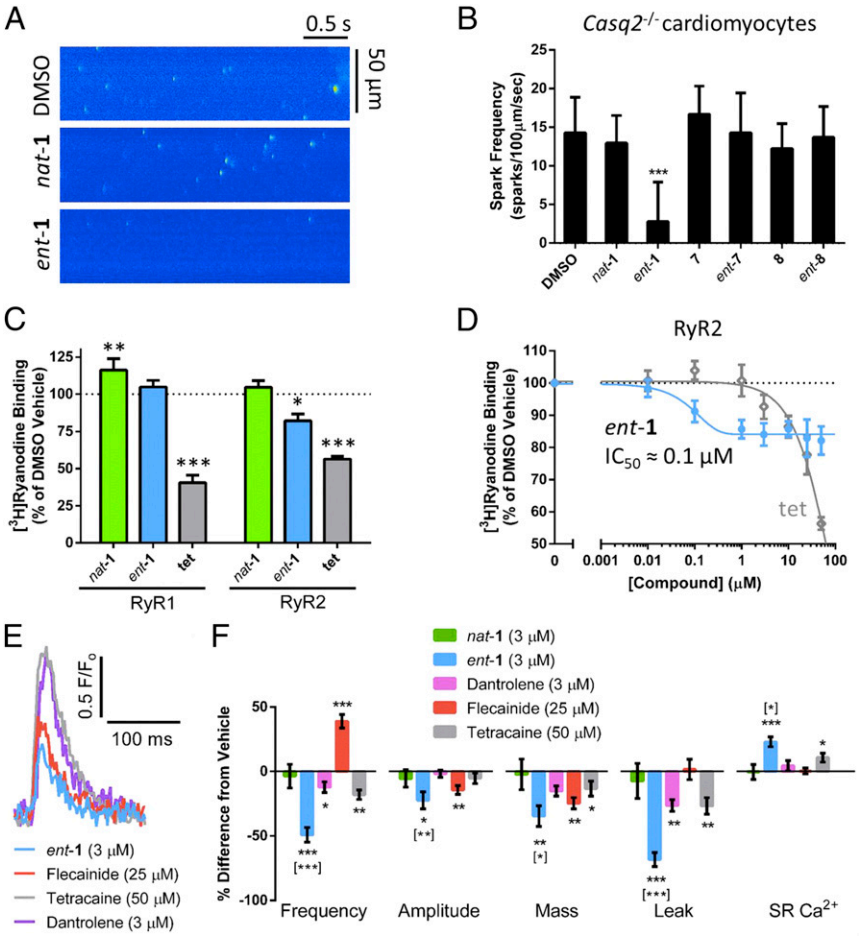

Fig. 2. Ca^{2+} spark and [^{3}H]ryanodine binding measurements of RyR activity. (*A*) Representative confocal line scans of Ca^{2+} sparks in the absence (DMSO) or presence of 25 μM *nat*-**1** or *ent*-**1** in permeabilized $Casq2^{-/-}$ cardiomyocytes. (*B*) Ca^{2+} spark frequency in $Casq2^{-/-}$ cells treated with 25 μM *nat*-**1**, **7**, and **8** and their respective enantiomers. (*C*) Comparison of [^{3}H]ryanodine binding to sarcoplasmic reticulum (SR) isolated from porcine longissimus dorsi (RyR1) or cardiac ventricle (RyR2) in the presence of 50 μM *nat*-**1**, *ent*-**1**, or tetracaine (tet). (*D*) Dose–response curves for *ent*-**1** and tet inhibition of [^{3}H]ryanodine binding to RyR2. (*E*) Representative Ca^{2+} spark amplitudes from permeabilized wild-type cardiomyocytes treated with 3 μM *ent*-**1**, 25 μM flecainide, 50 μM tetracaine, or 3 μM dantrolene. (*F*) Percent change in spark frequency, amplitude, mass, leak, and SR Ca^{2+} content relative to vehicle (DMSO), obtained from wild-type myocytes. SR Ca^{2+} content was measured as the Ca^{2+} transient amplitude elicited by application of 10 mM caffeine ($n \geq 5$ cells per group). Data are presented as mean ± SEM. $n \geq 30$ cells per group for *A*, *B*, and *F*. $n = 4$ replicates for each concentration tested in *C* and *D*. $^*P < 0.05$ vs. DMSO, $^{**}P < 0.01$ vs. DMSO, $^{***}P < 0.001$ vs. DMSO by one-way ANOVA with Tukey's post hoc test (*B*) or *t* test (*C*, *D*, and *F*). Bracketed asterisks indicate *t* test comparison between *ent*-**1** and dantrolene.

ent-**1** inhibits RyR2-mediated Ca^{2+} release. Cardiac SR Ca^{2+} release is sensitive to the Ca^{2+} concentration present at the cytosolic face of RyR2 (38). Importantly, none of the compounds altered $[Ca^{2+}]_{free}$ (*SI Appendix*, Fig. S1). RyR2 activity is strongly regulated by the RyR2 interacting proteins calmodulin (CaM) and FKBP12.6 and by PKA and CaMKII phosphorylation (39). Utilizing an established in vitro assay (20), we determined that *ent*-**1** does not alter CaM and FKBP12.6 binding to RyR2 (*SI Appendix*, Fig. S2). We next quantified phosphorylation of the PKA consensus site RyR2-S2808 and the CaMKII consensus site RyR2-S2814, which were also not significantly altered by *ent*-**1** (*SI Appendix*, Fig. S3). To determine the functional effects and isoform specificity of *nat*-**1** and *ent*-**1** verticilide on RyRs, we carried out [^{3}H]ryanodine binding assays to SR vesicles isolated from skeletal (RyR1) and cardiac (RyR2) porcine muscle. [^{3}H]ryanodine binding to SR samples provides a well-established biochemical index of RyR opening (20). Skeletal and cardiac SR samples were incubated with 50 μM *nat*-**1**, *ent*-**1**, and tetracaine for 3 h. Results indicate that *nat*-**1** increases RyR1 activity but has no effect on RyR2 (Fig. 2*C*). In contrast, *ent*-**1** inhibits RyR2 but has no effect on RyR1. As a control, we used the well-established pan-RyR inhibitor, tetracaine, which inhibited both isoforms in these experiments, as expected (Fig. 2*C*). *ent*-**1** was selected to generate full dose–response curves for both cardiac (Fig. 2*D*) and skeletal (*SI Appendix*, Fig. S4) SR. *ent*-**1** inhibited RyR2 in a concentration-dependent manner with an apparent IC_{50} of ∼0.1 μM and maximal inhibition of ∼20% (Fig. 2*D*) but had no effect on RyR1 up to 50 μM (*SI Appendix*, Fig. S4). *ent*-**1** was a significantly more potent RyR2 inhibitor than the nonselective RyR inhibitor tetracaine (Fig. 2*D*).

We next tested the effect of *ent*-**1** on Ca sparks in cardiomyocytes isolated from wild-type mice (Fig. 2 *E* and *F*) and from mice homozygous for the RyR2-R4496C mutation (*SI Appendix*, Fig. S5), which causes CPVT in humans. In both wild-type and mutant RyR2, 3 μM *ent*-**1** had a dual effect on Ca^{2+} sparks: a significant reduction in the rate of spontaneous Ca^{2+} sparks (reported as spark frequency) and the amount of Ca^{2+} released during each Ca^{2+} spark (measured as spark amplitude and spark mass; Fig. 2*F* and *SI Appendix*, Fig. S5). As a result, Ca^{2+} spark-mediated SR Ca^{2+} leak was drastically reduced (Fig. 2*F*). Notably, when applied at the same concentration, *ent*-**1** inhibited Ca^{2+} sparks with significantly higher efficacy than the nonselective RyR inhibitor dantrolene (Fig. 2*F*). Moreover, the effect of *ent*-**1** on spark parameters was distinct from that of other RyR inhibitors: *ent*-**1** significantly reduced spark amplitude (analogous to flecainide), whereas dantrolene and tetracaine did not. The effects of *ent*-**1** on Ca^{2+} spark frequency were similar to dantrolene and tetracaine but different from flecainide, which causes a paradoxical increase in spark frequency, as previously reported (40). As a result, *ent*-**1** reduced Ca^{2+} leak significantly more than dantrolene, tetracaine, or flecainide. Taken together, our results demonstrate that *ent*-**1** is not only significantly more potent (lower IC_{50}) but also has superior efficacy as a Ca^{2+} spark inhibitor compared with dantrolene, flecainide, and tetracaine.

nat-**1** can cross cellular membranes, based on its documented insecticidal activity and insect RyR inhibition. To test whether *ent*-**1** crosses the sarcolemma (muscle plasma membrane), we measured spontaneous Ca^{2+} release in intact $Casq2^{-/-}$ cardiomyocytes. Isolated cardiomyocytes were incubated with isoproterenol to stimulate adrenergic activation and a CPVT-like

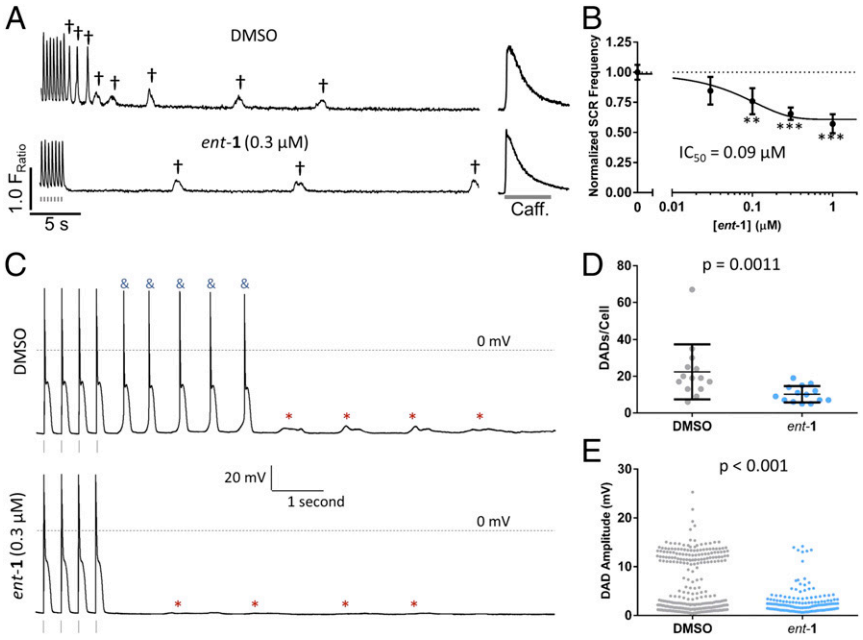

Fig. 3. Spontaneous Ca^{2+} release (SCR) and membrane potential recordings in single-cell $Casq2^{-/-}$ cardiomyocytes. (*A*) Isolated cardiomyocytes were field-stimulated at 3 Hz for 20 s followed by 40 s recording of SCR events (†). Application of 10 mM caffeine (caff) was used to measure SR Ca^{2+} content. (*B*) SCR frequency following cessation of pacing. n = 63, 27, 31, 63, and 30 cells for 0, 0.03, 0.1, 0.3, and 1.0 μM *ent*-**1**, respectively. $^{**}P < 0.01$, $^{***}P < 0.001$ vs. DMSO by t test. (*C*) Representative membrane potential recordings from current-clamped cardiomyocytes stimulated at 3 Hz for 20 s (last five stimulated beats are indicated) followed by 40 s recording of spontaneous activity. Dotted line indicates 0 mV. DADs are indicated by * and &, which sometimes generate triggered beats (&). (*D*) Total DADs per cell. (*E*) DAD amplitude for each event. Data are presented as mean ± SD. n = 14 cells in each group. P values calculated using Mann–Whitney U test.

cellular phenotype consisting of spontaneous Ca^{2+} release events (Fig. 3*A*). *ent*-**1** significantly reduced the frequency of spontaneous Ca^{2+} release (Fig. 3*B*), suggesting that *ent*-**1** is able to cross the sarcolemma and exert biological activity. Inhibition of spontaneous Ca^{2+} release displays potency similar to that observed in the [^{3}H]ryanodine binding assay (Fig. 2 *C* and *D*) but with greater biological efficacy. Consistent with inhibition of RyR2-mediated Ca^{2+} release, *ent*-**1** reduced diastolic Ca^{2+} levels in the cytoplasm, decreased Ca^{2+} transient amplitude, and delayed time-to-peak of paced transients (*SI Appendix*, Fig. S6). *ent*-**1** did not alter SR Ca^{2+} content (*SI Appendix*, Fig. S6*B*) or Ca^{2+} decay kinetics, a measure of SERCA function (4), which mediates Ca^{2+} uptake into the SR (*SI Appendix*, Fig. S6*F*); *ent*-**1** also did not alter L-type Ca currents (*SI Appendix*, Fig. S7), which are responsible for Ca^{2+} influx into the cell during excitation contraction coupling (8). Taken together, the results indicate that reduced Ca influx, reduced SR load, or impaired Ca^{2+} reuptake do not account for the reduction in spontaneous Ca^{2+} release by *ent*-**1**.

Spontaneous Ca^{2+} release activates the electrogenic Na–Ca exchanger (NCX) (8). The resulting inward NCX current produces cell membrane depolarizations that are referred to as delayed afterdepolarizations (DADs) (41). DADs can trigger premature beats that evoke ventricular ectopy and arrhythmogenesis (42). Hence, we next determined if *ent*-**1** inhibits DADs and triggered action potentials in patch-clamped $Casq2^{-/-}$ cardiomyocytes. DADs and triggered action potentials were elicited by a 3-Hz pacing train (Fig. 3*C*). *ent*-**1** (0.3 μM) significantly reduced both the frequency and amplitude of DADs (Fig. 3 *C*–*E*). Moreover, *ent*-**1** almost completely prevented DADs of large amplitude (i.e., >10 mV; Fig. 3*E*), which was likely responsible for the large reduction of triggered action potentials (7.7 vs. 0.4, $P = 0.01$). At the same time, *ent*-**1** had no significant effects on the duration or shape of the cardiac action potential (*SI Appendix*, Fig. S8), indicating that *ent*-**1** does not inhibit membrane ion channels. *ent*-**1** also did not inhibit the NCX directly, as evidenced by its lack of an effect on the decay rate of caffeine-induced Ca transients (*SI Appendix*, Fig. S6*G*), which is an established measure of NCX activity (39). Taken together, these results indicate that *ent*-**1** inhibits DADs and triggered action potentials in intact cardiomyocytes by selective inhibition of RyR2-mediated Ca release.

We next determined whether *ent*-**1** inhibition of Ca^{2+} release and DADs in cardiomyocytes in vitro translates into activity against catecholamine-induced ventricular arrhythmia in vivo. Fig. 4*A*

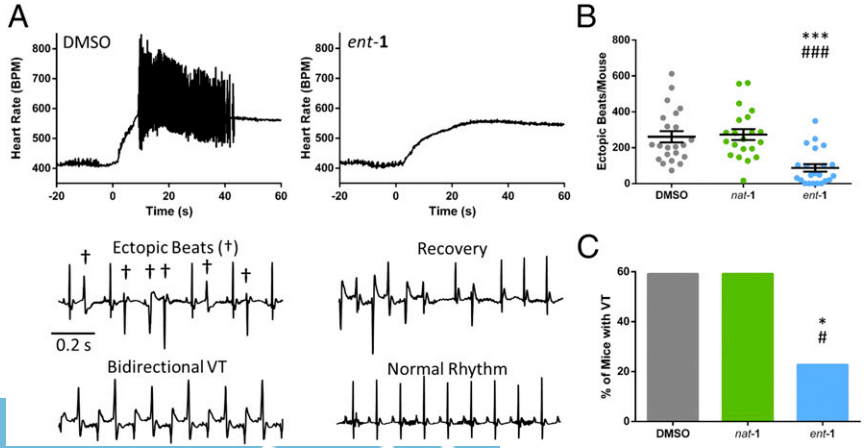

Fig. 4. *ent*-**1** inhibition of ventricular arrhythmia in mice. (*A*) Representative heart rate traces in $Casq2^{-/-}$ mice treated with DMSO or *ent*-**1**. Isoproterenol (3.0 mg/kg i.p.) was injected at 0 s. Rhythm strips show arrhythmia features. Ectopic beats (†) produce a variable HR in the traces. (*B*) Quantification of catecholamine-induced ectopic beats by surface electrocardiogram in $Casq2^{-/-}$ mice injected intraperitoneally with 30 mg/kg (drug/body weight) *nat*-**1** or *ent*-**1** or DMSO of equivalent volume 30 min before recordings. $^{***}P < 0.001$ vs. DMSO or $^{\#\#\#}P < 0.001$ vs. *nat*-**1** by Mann–Whitney U test. (*C*) Incidence of ventricular tachycardia (VT). $^{*}P = 0.0305$ for *ent*-**1** vs. DMSO or $^{\#}P = 0.0305$ for *ent*-**1** vs. *nat*-**1** by Fisher's exact test. n = 22 mice per group (*B* and *C*). Data in *B* are presented as mean ± SEM.

(first panel) illustrates the HR response to isoproterenol (0 s) and subsequent development of ventricular arrhythmias. *ent*-**1** significantly reduced the number of ventricular ectopic beats (Fig. 4 *A* and *B*), primarily in the form of premature ventricular complexes. *ent*-**1** also reduced the incidence of ventricular tachycardia (Fig. 4*C*), an established risk factor for sudden cardiac death (41).

Although there were no differences in baseline heart rate (HR) before isoproterenol, *ent*-**1** significantly reduced peak HR and, consequently, ΔHR after isoproterenol injection (*SI Appendix*, Fig. S9). The HR reduction by *ent*-**1** is consistent with its inhibition of RyR2 channels in the sinoatrial node and hence the intracellular Ca^{2+} clock responsible for HR acceleration in response to catecholamines (43). To exclude the possibility that the reduction in peak HR was responsible for the arrhythmia reduction by *ent*-**1**, we used a linear regression model to assess whether lower peak HR or ΔHR confer protection from ectopic beats. No association was found between peak or ΔHR and the number of ectopic beats in the DMSO and *nat*-**1** groups (*SI Appendix*, Fig. S9 *D–F*). Hence, RyR2 inhibition by *ent*-**1**, rather than reduced peak HR or ΔHR, is responsible for the reduction in ectopic beats evinced by *ent*-**1**. Drugs that block cell membrane Na^+ or L-type Ca^{2+} channels can prevent CPVT (44). To assess whether *ent*-**1** in vivo efficacy was a result of Na^+ channel or Ca^{2+} channel block, we measured the ECG QRS duration (prolonged by Na^+ channel blockers) and the PR interval (prolonged by Ca^{2+} channel blockers). Consistent with its lack of effect on the cardiac action potential in single cells (*SI Appendix*, Fig. S8), *ent*-**1** had no significant effect on QRS or PR interval (*SI Appendix*, Fig. S10), indicating that Na^+ or Ca^{2+} channel block by *ent*-**1** does not contribute to its antiarrhythmic activity in vivo.

Conclusion

Our current investigation led us to examine the effects of a known insect RyR modulator, *nat*-(−)-verticilide, two synthetic precursors, and their mirror image isomers (*ent*). Surprisingly, whereas natural verticilide had no effect on mammalian RyR2, we found that its enantiomer significantly inhibited RyR2-mediated Ca^{2+} leak by a distinct MOA compared with other RyR2 inhibitors. *ent*-**1** significantly attenuated spontaneous Ca^{2+} release in cardiomyocytes isolated from two CPVT mouse models and from wild-type mice. The combined reduction of Ca^{2+} spark frequency, amplitude, and mass resulted in a greater reduction of Ca^{2+} leak in the presence of *ent*-**1** (Fig. 2) compared with the benchmark compounds dantrolene, tetracaine, and flecainide. The dual and potent reduction of both spark frequency and spark mass suggests that *ent*-**1** may be a prototype of a new class of RyR2 modulators, which could have superior activity against ventricular arrhythmias triggered by RyR2-mediated Ca^{2+} release. Furthermore, *ent*-**1** in vivo efficacy establishes it as a promising lead compound for developing small-molecule therapeutics aimed at suppressing Ca^{2+} leak, with potential use in CPVT, heart failure, atrial fibrillation, and neurological disorders.

To probe the relationship between molecular structure and Ca^{2+} spark suppression, we tested the effects of each enantiomer of verticilide and its linear and desmethyl cyclic precursors. Our finding that *ent*-**1** significantly decreased spontaneous Ca^{2+} leak but *nat*-**1** did not have any effect suggests that there is a specific ligand–receptor interaction between *ent*-**1** and a chiral binding site in the cell. Enantiomer-dependent inhibition of RyR2-mediated Ca^{2+} release has also been reported for the drug propafenone, which has antiarrhythmic properties similar to flecainide and is clinically used in racemic form (45). Compared with *S*-propafenone, *R*-propafenone is a significantly more potent inhibitor of RyR2 single channels in artificial bilayers (45) and Ca^{2+} sparks in cardiomyocytes (14). Similar to *nat*-**1**, the N–H (**8**) and linear (**7**) congeners (and their enantiomers) did not exhibit an inhibitory effect. Hence, the cyclic form of *ent*-**1** is also essential for activity. The amino acid sequence of insect RyR only shares about 45% homology with the mammalian isoforms (46). The carboxyl-terminal portion of insect RyR, which forms the pore region of the Ca^{2+} release channel, is highly conserved with over 90% homology with the corresponding region of the mammalian isoforms (46). However, insect and mammalian RyR isoforms differ greatly in the large amino-terminal portion of the channel, which extends into the cytosol and contains multiple binding sites for Ca^{2+} release channel modulators (46). These regions of high divergence are possible candidates for *ent*-**1** interaction with mammalian RyR2 and should, therefore, be the initial focus of future efforts to locate this compound's binding site within the RyR2 structure. It is unknown whether *ent*-**1** binds to insect RyR; however, the lack of effect of *nat*-**1** on mammalian RyR2 is reassuring for developing it and its congeners as insecticides (34).

Importantly, RyR2 inhibition by *ent*-**1** saturates at less than 100% (Figs. 2 and 3). This confers safety for therapeutic use in vivo because full RyR2 inhibition would block muscle contraction and thus be lethal. Similar partial inhibition has been observed with other RyR modulators, e.g., the pan-RyR inhibitor dantrolene (47), or with accessory proteins FKBP12.0 and 12.6 (48), calmodulin, or S100A1 (20). The most plausible explanation for the partial inhibition is that *ent*-verticilide functions as a negative allosteric modulator; that is, it does not block the channel pore. Although further studies are needed to identify the exact binding site, the observed inhibition of [^{3}H]ryanodine binding and RyR2 Ca sparks suggests that *ent*-**1** acts by directly binding to the RyR2 channel complex. Consistent with that interpretation, *ent*-**1** had no effect on RyR2 phosphorylation by PKA or Ca^{2+}-CaM Kinase II or on binding of the RyR2 accessory proteins CaM and FKBP12.6, all of which have been shown to regulate RyR2 activity (49). Furthermore, our report highlights a rare and exciting discovery of an unnatural enantiomer that potently inhibits RyR2-mediated Ca^{2+} leak, whereas the natural product is completely inactive. Due to synthetic barriers, there are few instances where the biological activity of an unnatural enantiomer can be studied in comparison with its naturally occurring analog (50–59). Within these instances, the unnatural enantiomer is generally found to be comparably potent to the natural product, (52–57), and there are a select few examples where the unnatural enantiomer is modestly more potent than the natural product (58, 59). However, this discovery is unique because to the best of our knowledge, there are no examples where the unnatural enantiomer of a COD natural product is highly potent in a biological system while the natural enantiomer is inactive. The straightforward synthetic methods to complex cyclodepsipeptides outlined here overcome the common shortcomings that previously limited their accessibility, as demonstrated by the enantiomer-specific preparations of *nat*-**1** and the heretofore unknown *ent*-**1**. Our ability to access the unnatural—or "dark"—enantiomer and discovery of its activity raises the question whether similar dark chemical space holds generally untapped potential. In the case of verticilide, the unnatural enantiomer induces a pharmacological behavior similar but mechanistically orthogonal to existing Ca^{2+} release inhibitors flecainide and tetracaine, whereas the natural product is inactive. This discovery not only confirms the importance of developing straightforward synthetic methods toward natural products and their derivatives but also contributes to the ongoing excitement to explore dark chemical space (24, 60) for chemical biology.

ACKNOWLEDGMENTS. This work was supported in part by National Institutes of Health (NIH) Grants T32 NS 007491 (to B.C.K. and D.J.B.), HL092097 (to R.L.C.), HL138539 (to R.L.C.), GM 063557 (to J.N.J.), HL128044 (to B.C.K.), HL124935 (to B.C.K.), HL088635 (to B.C.K.), and R35-HL144980 (to B.C.K.); a PhRMA Foundation Postdoctoral Fellowship (to D.J.B.); NIH Postdoctoral Fellowship F32-HL140874 (to D.J.B.); American Heart Association Postdoctoral Fellowship 16POST31010019 (to R.T.R.); and American Heart Association Atrial Fibrillation Strategically Focused Research Network Postdoctoral Fellowship 18SFRN34110369 (to K.K.). Ca^{2+} spark measurements were performed using the Vanderbilt University Medical Center Cell Imaging Shared Resource (supported by NIH Grants CA68485, DK20593, DK58404, DK59637, and EY008126).

1. Yuan Q, et al. (2016) Calstabin 2: An important regulator for learning and memory in mice. *Sci Rep* 6:21087.
2. Johnson JN, Tester DJ, Bass NE, Ackerman MJ (2010) Cardiac channel molecular autopsy for sudden unexpected death in epilepsy. *J Child Neurol* 25:916–921.
3. Lehnart SE, et al. (2008) Leaky Ca2+ release channel/ryanodine receptor 2 causes seizures and sudden cardiac death in mice. *J Clin Invest* 118:2230–2245.
4. Chen X, et al. (2011) Dantrolene is neuroprotective in Huntington's disease transgenic mouse model. *Mol Neurodegener* 6:81.
5. Wei H, Perry DC (1996) Dantrolene is cytoprotective in two models of neuronal cell death. *J Neurochem* 67:2390–2398.
6. Liu J, et al. (2009) Deranged calcium signaling and neurodegeneration in spinocerebellar ataxia type 2. *J Neurosci* 29:9148–9162.
7. Chen X, et al. (2008) Deranged calcium signaling and neurodegeneration in spinocerebellar ataxia type 3. *J Neurosci* 28:12713–12724.
8. Bers DM (2002) Cardiac excitation-contraction coupling. *Nature* 415:198–205.
9. Marks AR (2013) Calcium cycling proteins and heart failure: Mechanisms and therapeutics. *J Clin Invest* 123:46–52.
10. Knollmann BC, et al. (2006) Casq2 deletion causes sarcoplasmic reticulum volume increase, premature Ca2+ release, and catecholaminergic polymorphic ventricular tachycardia. *J Clin Invest* 116:2510–2520.
11. Loaiza R, et al. (2013) Heterogeneity of ryanodine receptor dysfunction in a mouse model of catecholaminergic polymorphic ventricular tachycardia. *Circ Res* 112: 298–308.
12. Kannankeril PJ, et al. (2006) Mice with the R176Q cardiac ryanodine receptor mutation exhibit catecholamine-induced ventricular tachycardia and cardiomyopathy. *Proc Natl Acad Sci USA* 103:12179–12184.
13. Watanabe H, et al. (2009) Flecainide prevents catecholaminergic polymorphic ventricular tachycardia in mice and humans. *Nat Med* 15:380–383.
14. Galimberti ES, Knollmann BC (2011) Efficacy and potency of class I antiarrhythmic drugs for suppression of Ca2+ waves in permeabilized myocytes lacking calsequestrin. *J Mol Cell Cardiol* 51:760–768.
15. Bannister ML, et al. (2015) The mechanism of flecainide action in CPVT does not involve a direct effect on RyR2. *Circ Res* 116:1324–1335.
16. Brunton LL, Hilal-Dandan R, Knollmann BC (2018) *Goodman and Gilman's the Pharmacological Basis of Therapeutics* (McGraw Hill Medical, New York), 13th Ed.
17. Oo YW, et al. (2015) Essential role of calmodulin in RyR inhibition by dantrolene. *Mol Pharmacol* 88:57–63.
18. Zhao F, Li P, Chen SRW, Louis CF, Fruen BR (2001) Dantrolene inhibition of ryanodine receptor Ca2+ release channels. Molecular mechanism and isoform selectivity. *J Biol Chem* 276:13810–13816.
19. Kobayashi S, et al. (2010) Dantrolene, a therapeutic agent for malignant hyperthermia, inhibits catecholaminergic polymorphic ventricular tachycardia in a RyR2(R2474S/+) knock-in mouse model. *Circ J* 74:2579–2584.
20. Rebbeck RT, et al. (2016) S100A1 protein does not compete with calmodulin for ryanodine receptor binding but structurally alters the ryanodine receptor·calmodulin complex. *J Biol Chem* 291:15896–15907.
21. Cheng H, Lederer WJ, Cannell MB (1993) Calcium sparks: Elementary events underlying excitation-contraction coupling in heart muscle. *Science* 262:740–744.
22. Newman DJ, Cragg GM (2016) Natural products as sources of new drugs from 1981 to 2014. *J Nat Prod* 79:629–661.
23. Finefield JM, Sherman DH, Kreitman M, Williams RM (2012) Enantiomeric natural products: Occurrence and biogenesis. *Angew Chem Int Ed Engl* 51:4802–4836.
24. Noguchi T, et al. (2016) Screening of a virtual mirror-image library of natural products. *Chem Commun (Camb)* 52:7653–7656.
25. Felício MR, Silva ON, Gonçalves S, Santos NC, Franco OL (2017) Peptides with dual antimicrobial and anticancer activities. *Front Chem* 5:5.
26. Süssmuth R, Müller J, von Döhren H, Molnár I (2011) Fungal cyclooligomer depsipeptides: From classical biochemistry to combinatorial biosynthesis. *Nat Prod Rep* 28: 99–124.
27. Rizo J, Gierasch LM (1992) Constrained peptides: Models of bioactive peptides and protein substructures. *Annu Rev Biochem* 61:387–418.
28. Heitz F, Kaddari F, Heitz A, Ranirisehenо H, Lazaro R (1989) Conformations, cation binding, and transmembrane ion transfer properties of a cyclooctapeptide built by an alternation of D and L residues. *Int J Pept Protein Res* 34:387–393.
29. Gao M, Cheng K, Yin H (2015) Targeting protein-protein interfaces using macrocyclic peptides. *Biopolymers* 104:310–316.
30. Villar EA, et al. (2014) How proteins bind macrocycles. *Nat Chem Biol* 10:723–731.
31. Feifel SC, et al. (2007) In vitro synthesis of new enniatins: Probing the alpha-D-hydroxy carboxylic acid binding pocket of the multienzyme enniatin synthetase. *ChemBioChem* 8:1767–1770.
32. Pieper R, Haese A, Schröder W, Zocher R (1995) Arrangement of catalytic sites in the multifunctional enzyme enniatin synthetase. *Eur J Biochem* 230:119–126.
33. Xu Y, et al. (2007) Cytotoxic and Antihaptotactic beauvericin analogues from precursor-directed biosynthesis with the insect pathogen Beauveria bassiana ATCC 7159. *J Nat Prod* 70:1467–1471.
34. Monma S, et al. (2006) Verticilide: Elucidation of absolute configuration and total synthesis. *Org Lett* 8:5601–5604.
35. Shiomi K, et al. (2010) Verticilide, a new ryanodine-binding inhibitor, produced by Verticillium sp. FKI-1033. *J Antibiot (Tokyo)* 63:77–82.
36. Ohshiro T, et al. (2012) New verticilides, inhibitors of acyl-CoA:cholesterol acyltransferase, produced by Verticillium sp. FKI-2679. *J Antibiot (Tokyo)* 65:255–262.
37. Batiste SM, Johnston JN (2016) Rapid synthesis of cyclic oligomeric depsipeptides with positional, stereochemical, and macrocycle size distribution control. *Proc Natl Acad Sci USA* 113:14893–14897.
38. Meissner G (1994) Ryanodine receptor/Ca2+ release channels and their regulation by endogenous effectors. *Annu Rev Physiol* 56:485–508.
39. Bers DM (2000) Calcium fluxes involved in control of cardiac myocyte contraction. *Circ Res* 87:275–281.
40. Hilliard FA, et al. (2010) Flecainide inhibits arrhythmogenic Ca2+ waves by open state block of ryanodine receptor Ca2+ release channels and reduction of Ca2+ spark mass. *J Mol Cell Cardiol* 48:293–301.
41. Knollmann BC, Roden DM (2008) A genetic framework for improving arrhythmia therapy. *Nature* 451:929–936.
42. Schlotthauer K, Bers DM (2000) Sarcoplasmic reticulum Ca(2+) release causes myocyte depolarization. Underlying mechanism and threshold for triggered action potentials. *Circ Res* 87:774–780.
43. Lakatta EG, Maltsev VA, Vinogradova TM (2010) A coupled SYSTEM of intracellular Ca2+ clocks and surface membrane voltage clocks controls the timekeeping mechanism of the heart's pacemaker. *Circ Res* 106:659–673.
44. Katz G, et al. (2010) Optimizing catecholaminergic polymorphic ventricular tachycardia therapy in calsequestrin-mutant mice. *Heart Rhythm* 7:1676–1682.
45. Hwang HS, et al. (2011) Inhibition of cardiac Ca2+ release channels (RyR2) determines efficacy of class I antiarrhythmic drugs in catecholaminergic polymorphic ventricular tachycardia. *Circ Arrhythm Electrophysiol* 4:128–135.
46. Xu X, Bhat MB, Nishi M, Takeshima H, Ma J (2000) Molecular cloning of cDNA encoding a drosophila ryanodine receptor and functional studies of the carboxyl-terminal calcium release channel. *Biophys J* 78:1270–1281.
47. Kobayashi S, et al. (2009) Dantrolene, a therapeutic agent for malignant hyperthermia, markedly improves the function of failing cardiomyocytes by stabilizing interdomain inter-actions within the ryanodine receptor. *J Am Coll Cardiol* 53:1993–2005.
48. Cornea RL, Nitu FR, Samsó M, Thomas DD, Fruen BR (2010) Mapping the ryanodine receptor FK506-binding protein subunit using fluorescence resonance energy transfer. *J Biol Chem* 285:19219–19226.
49. Van Petegem F (2012) Ryanodine receptors: Structure and function. *J Biol Chem* 287: 31624–31632.
50. Hung DT, Nerenberg JB, Schreiber SL (1994) Distinct binding and cellular properties of synthetic (+)- and (-)-discodermolides. *Chem Biol* 1:67–71.
51. Siddiqi SM, et al. (1994) Antiviral enantiomeric preference for 5′-norariste romycin. *J Med Chem* 37:551–554.
52. Logan MM, Toma T, Thomas-Tran R, Du Bois J (2016) Asymmetric synthesis of batrachotoxin: Enantiomeric toxins show functional divergence against Na_V. *Science* 354:865–869.
53. Wade D, et al. (1990) All-D amino acid-containing channel-forming antibiotic peptides. *Proc Natl Acad Sci USA* 87:4761–4765.
54. Tichenor MS, et al. (2006) Asymmetric total synthesis of (+)- and ent-(-)-yatakemycin and duocarmycin SA: Evaluation of yatakemycin key partial structures and its unnatural enantiomer. *J Am Chem Soc* 128:15683–15696.
55. Iwasa E, et al. (2010) Total synthesis of (+)-chaetocin and its analogues: Their histone methyltransferase G9a inhibitory activity. *J Am Chem Soc* 132:4078–4079.
56. Sando L, et al. (2011) A synthetic mirror image of kalata B1 reveals that cyclotide activity is independent of a protein receptor. *Chembiochem* 12:2456–2462.
57. Boger DL, Johnson DS (1995) CC-1065 and the duocarmycins: Unraveling the keys to a new class of naturally derived DNA alkylating agents. *Proc Natl Acad Sci USA* 92: 3642–3649.
58. Boger DL, Hong J (2001) Asymmetric total synthesis of ent-(-)-roseophilin: Assignment of absolute configuration. *J Am Chem Soc* 123:8515–8519.
59. Farmer RL, Scheidt KA (2013) A concise enantioselective synthesis and cytotoxic evaluation of the anticancer rotenoid deguelin enabled by a tandem knoevenagel/conjugate addition/decarboxylation sequence. *Chem Sci (Camb)* 4:3304–3309.
60. Wassermann AM, et al. (2015) Dark chemical matter as a promising starting point for drug lead discovery. *Nat Chem Biol* 11:958–966.